Supplementary material

Structure of the complex between teicoplanin and a bacterial cell-wall peptide: Use of a carrier protein approach

Economou, N.J., Lazo, E.O., Jaconcic, J., Zentner, I.J., Grasty, K.C., Weeks, S.D., Cocklin, S., Stojanoff, V., Loll, P.J.

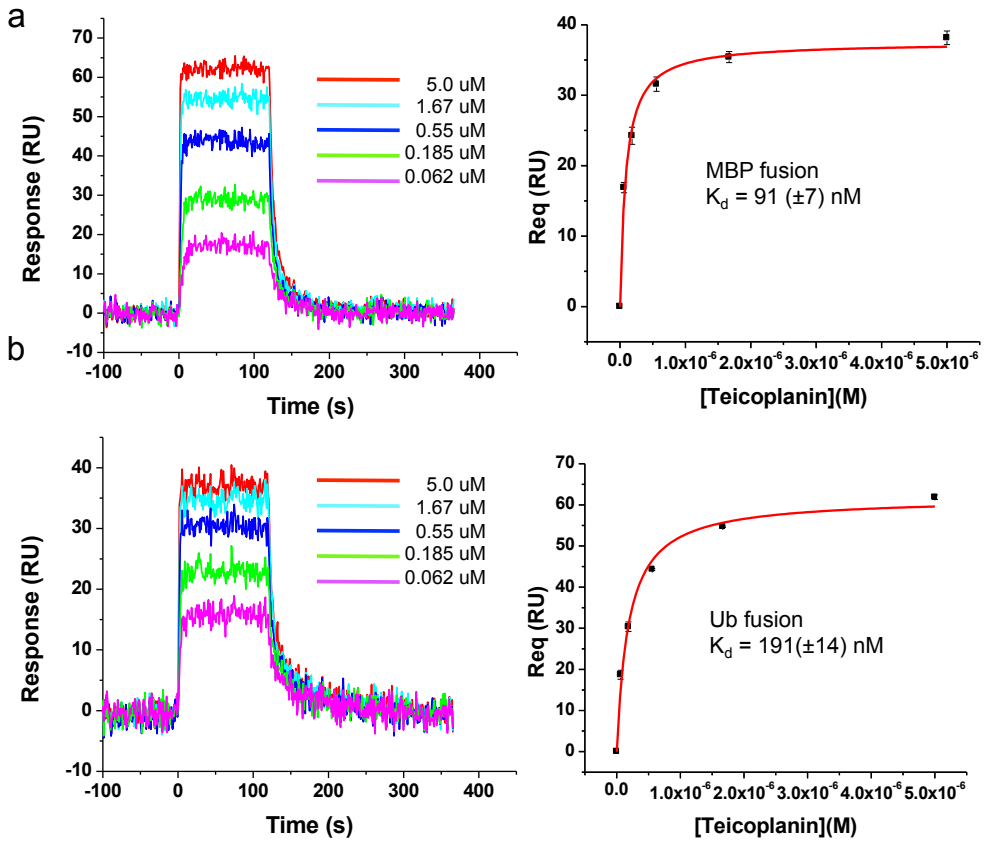

Figure S1. *SPR analysis of teicoplanin binding to carrier protein-peptide fusions*. (*Left)* Representative sensorgrams for teicoplanin binding to immobilized carrier protein-peptide fusions. Panel (a) shows the MBP-peptide fusion, and panel (b) shows the ubiquitin-peptide fusion. The sensorgrams shown have been corrected for nonspecific binding. The different color sensorgrams correspond to the different concentrations shown for the teicoplanin analyte *(Right)* Binding curves corresponding to the sensorgrams shown at left. K_D (± SE) values shown are averages of triplicate experiments. Error bars present one standard deviation. Req, response at equilibrium; RU, response units.

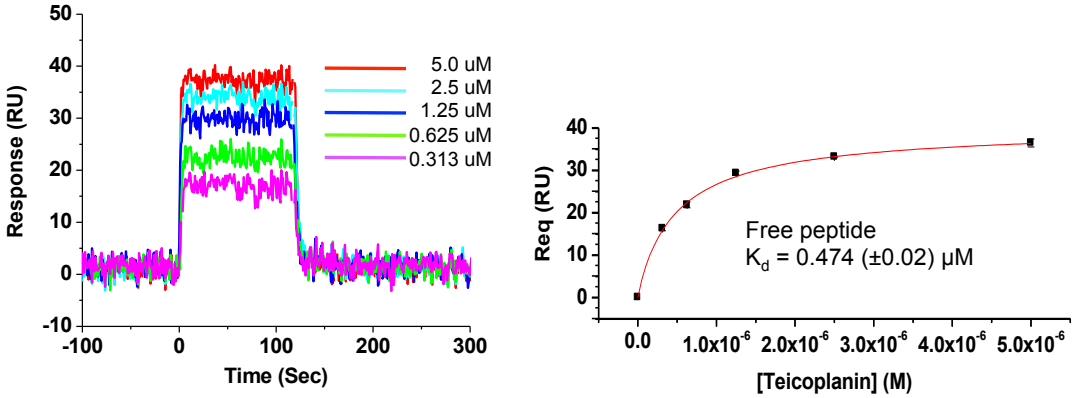

Figure S2. *SPR analysis of teicoplanin binding to its target peptide alone*. (*Left)* Representative sensorgrams for teicoplanin binding to immobilized Cys-Lys-D-Ala-D-Ala peptide. The sensorgrams shown have been corrected for nonspecific binding. The different color sensorgrams correspond to the different concentrations shown for the teicoplanin analyte *(Right)* Binding curves corresponding to the sensorgrams shown at left. K_D (± SE) values shown are averages of triplicate experiments. Error bars present one standard deviation. Req, response at equilibrium; RU, response units.

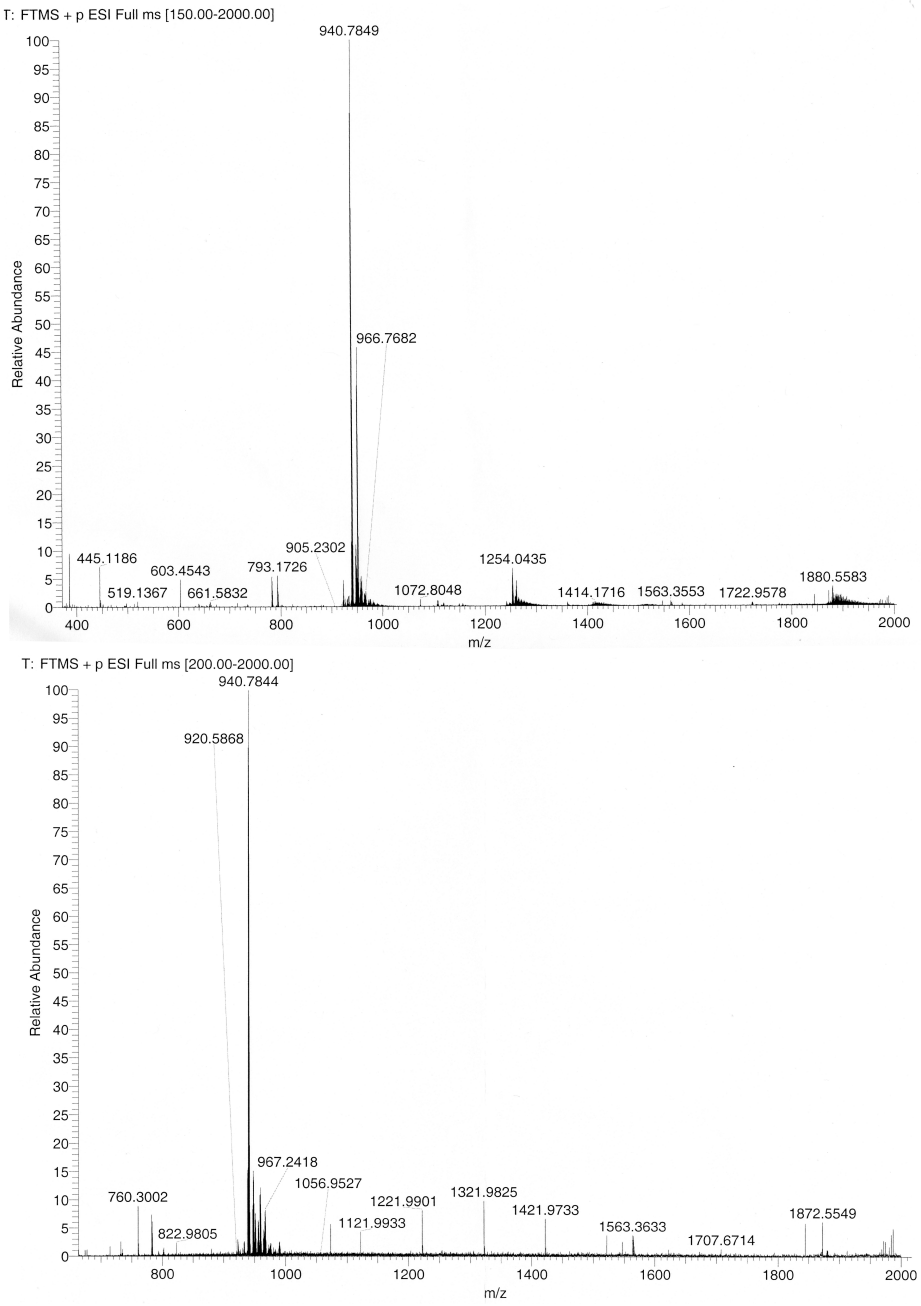

Figure S3. *Mass spectra of dissolved MBP-teicoplanin crystals. Upper panel)* Spectrum from dissolved crystals. *Lower panel*) Mass spectrum of the teicoplanin starting material. Crystals of the complex were rinsed exhaustively with protein- and teicoplanin-free mother liquor, dissolved in nuclease-free water, and subsequently analyzed with ESI mass spectrometry (NIH/NCRR Mass Spectrometry Resource, Washington University). The predicted m/z ratio for the doubly charged $[M+2H]^{2+}$ ion is 940.8, while the predicted m/z ratio for the corresponding mono-dechloro species would be 923.6 (teicoplanin nominal mass = 1879.66 Da).

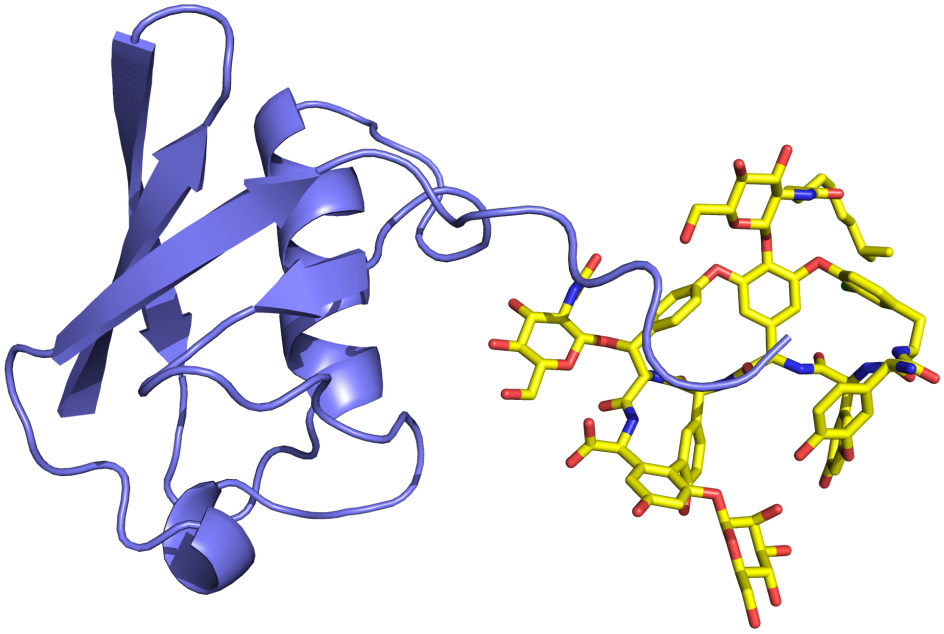

Figure S4. *Structure of the ubiquitin-peptide fusion in complex with teicoplanin*. The backbone of the ubiquitin-peptide fusion is shown in a blue cartoon representation; the teicoplanin is shown in a stick representation, with the following color code: yellow, carbon; red, oxygen; blue, nitrogen.

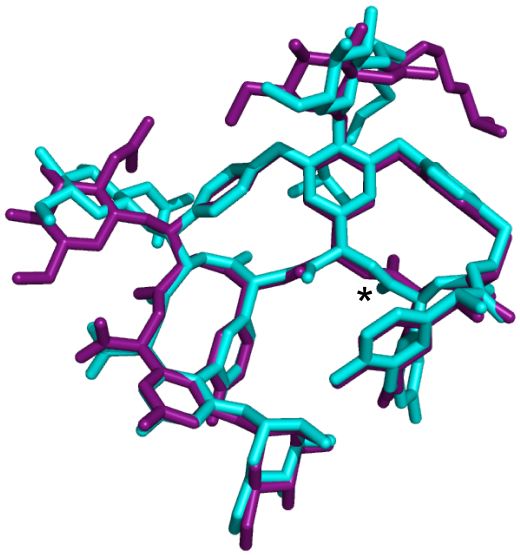

Figure S5. *Superposition of the two teicoplanin structures determined using the carrier protein strategy*. Stick representations are shown for teicoplanin bound to the MBP-peptide fusion (cyan) and to the ubiquitin-peptide fusion (purple). The position of the carbonyl group of residue 3 is marked with an asterisk.

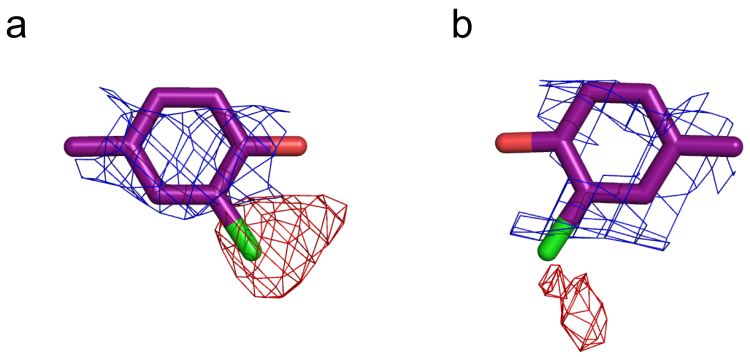

Figure S6. *Dechlorination of the antibiotic in ubiquitin-teicoplanin crystals*. Panel (a) shows the side chain of residue 6; panel (b) shows the side chain of residue 3. A 2Fo-Fc omit-map is shown in blue, contoured at 0.5 sigma. Also shown is an Fo-Fc map, with negative density colored red and contoured at -3 sigma. The chlorine atoms are shown in green, carbon atoms are colored purple, and oxygen red.

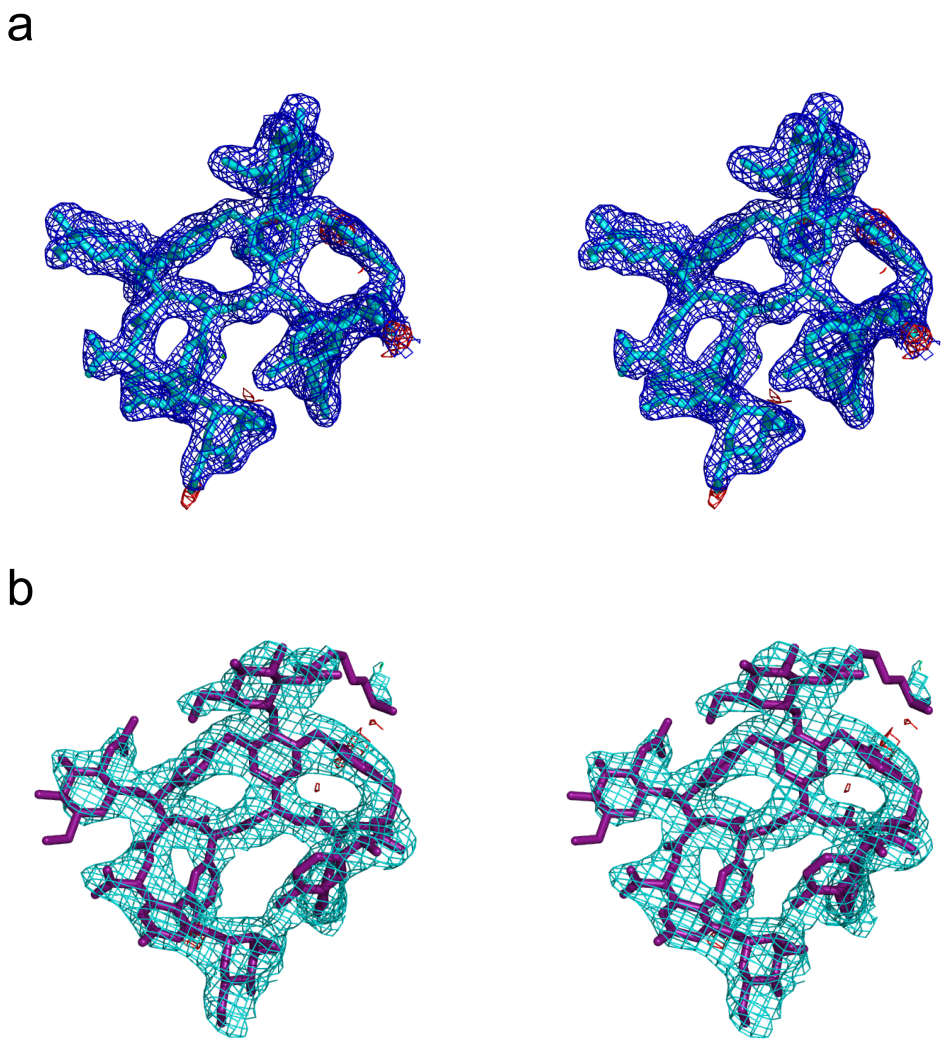

Figure S7. Stereoviews of the electron density for teicoplanin in complex with the MBP-Ala_5-peptide fusion (*a*) and the ubiquitin-peptide fusion (*b*). 2Fo-Fc maps are contoured at 1.0 sigma, and are shown in blue in panel (*a*) and cyan in panel (*b*). Fo-Fc maps are shown in both panels contoured at +3 sigma (green) and -3 sigma (red).